journal

J. Am. Ceram. Soc., 93 [3] 887–893 (2010)
DOI: 10.1111/j.1551-2916.2009.03506.x

Facile Synthesis, Characterization of ZnO Nanotubes and Nanoflowers in an Aqueous Solution

Dewei Chu,† Yoshitake Masuda, Tatsuki Ohji, and Kazumi Kato

National Institute of Advanced Industrial Science and Technology (AIST), Moriyama-ku, Nagoya 463-8560, Japan

Two kinds of different ZnO nanostructures, nanotubes, and nanoflowers were synthesized using an aqueous solution approach. It was demonstrated that the addition of Al^{3+} and ZnO sol causes the different growth behavior of ZnO nanostructures, and leads to the formation of a nanotube array as well as self-assembled nanoflowers, respectively. The effects of reaction parameters on the morphology of ZnO nanostructures were investigated. The present route reports the possibility for morphology control and assembly of ZnO nanostructures on arbitrary substrates at a low temperature on a large scale.

I. Introduction

ZINC oxide (ZnO) is an *n*-type semiconductor that shows promise for a number of applications including transparent conductors and sensors.[1–3] Recently, owing to its size- and shape-dependent properties, nanostructured ZnO has been widely used in electronic and photoelectronic devices.[4–7] The performance of these devices depends critically on the morphology and dimension of ZnO nanostructures, which determine the electrical and thermal transport properties in addition to the optical and mechanical properties.[8–11]

So far, various ZnO nanostructures, such as nanowires, nanorod, and nanosheet, have been investigated in solar cells and biosensors.[12–15] For these applications, vertically well-aligned ZnO nanorod arrays, which have a large surface-to-volume ratio, have been extensively studied because the nanorod array morphology provides more direct conduction paths for electrons to transport from the point of injection to the collection electrode.[16] Usually, a high porosity and a large surface area are required to improve the efficiency and activity. Decreasing the nanorod diameter is one effective way to increase the specific surface area of ZnO. However, a smaller crystal size usually results in very high resistivity due to the abundance of grain boundary among nanorods. Alternatively, ZnO hollow nanostructures can contribute simultaneously to the extension of porosity and surface area as well as good electrical conductivity. Among them, ZnO nanotube arrays are of particular interest because of their unique physical and chemical properties.[17–22] As to the fabrication of ZnO nanotubes, a facile way is selective dissolution of the nanorod core in an aqueous solution.[19] The selective dissolution is caused by the fact that for hexagonal-shaped ZnO rods with well-defined (0001) and (1010) surfaces, the chemical activities of (0001) and (1010) surfaces are quite different. Besides, it was found that the feasibility of forming nanotubes is sensitive to the diameter of ZnO rods.[23] Consequently, electrodeposition is applied to precisely control the shape and the diameter of ZnO nanorods, followed by a chemical etching process to obtain tubular structures.[21] However, the application of electrodeposition is limited due to the requirement of a conductive substrate. Basically, the chemical bath deposition process is similar to that of electrodeposition, which involves deposition of ZnO onto an existing template via hydrolysis and condensation reactions of Zn^{2+} ions from solution. Vayssieres *et al.*[22] have demonstrated, in a Zn^{2+} amino complex system, that ZnO nanotubes could be fabricated after an extremely long time. Until now, the relationship between the growth condition and the structure of ZnO nanotubes was seldom reported, and facile ways to prepare ZnO nanotubes are still being explored.

Besides the electrical conductivity, the assembly of ZnO nanorods is also important because it plays a key role in enhancing dye loading and light harvesting. In fact, a nanorod array may be not favorable for light harvesting because some photons may not be absorbed by the dye interfacing ZnO.[16] Instead, as a novel nanostructure, in ZnO nanoflowers, the random branches of the nanoflowers benefit both a larger surface area and increased light–dye interactions.[24–28] However, most of the reported ZnO nanoflowers are randomly dispersed, not well assembled, and show poor electrical conductivity. Therefore, the controlled synthesis of ZnO nanoflowers as well as their assembly into large three-dimensional (3D) arrays on various types of substrates represent important tasks to fulfill the requirement of novel devices.

Here, we present a new strategy for fabricating arrays of ZnO nanotubes and nanoflowers in an aqueous solution with tailored dimensions; the formation of these two kinds of nanostructures is promoted by simply introducing additives into the reaction solution.

II. Experimental Procedure

All chemicals (Wako Pure Chemical Industries Ltd., Osaka, Japan) were used as received without further purification. Slide glass and FTO glass were used as substrates.

(1) Seed Layer Preparation

A ZnO seed was prepared using a modified sol–gel method. Basically, 1.1 g $Zn(CH_3COOH)_2 \cdot 2H_2O$ and 0.29 g $LiOH \cdot H_2O$ were dissolved into 50 mL ethanol, respectively. They were mixed rapidly, and stirred at 80°C for 10 min, and then cooled to room temperature. The resultant sol was transparent with ZnO nanoparticles, and the average size was around 3.5 nm.[29] The solution was then spin coated on the substrate at 500 rpm for 5 s and at 3000 rpm for 30 s. After processing, the substrate was heated at 100°C for 30 min to remove the solvent.

(2) Preparation of ZnO Nanotubes

Growth of a ZnO nanotube was carried out by suspending the substrate (slide glass) in a 40 mL beaker filled with an equimolar aqueous solution of 0.1*M* zinc nitrate hydrate ($Zn(NO_3)_2 \cdot 6H_2O$), 0.002*M* aluminum nitrate hydrate ($Al(NO_3)_3 \cdot 9H_2O$), and 0.1*M* methenamine ($C_6H_{12}N_4$) at 70°C for 3 h; the initial pH value of the solution was about 5.9–6.1. Subsequently, the substrate was removed from the solution, rinsed with deionized water, and immersed into 0.3*M* KOH aqueous solution at 80°C for

W.-C. Wei—contributing editor

Manuscript No. 26641. Received August 23, 2009; approved October 22, 2009.
†Author to whom correspondence should be addressed. e-mail: dewei-chu@aist.go.jp

1 h. Finally, the substrate was washed by deionized water and dried at 100°C for 1 h.

(3) Growth of ZnO Nanoflowers

For ZnO nanoflowers, 40 mL equimolar aqueous solution of 0.1*M* zinc nitrate hydrate, 0.1*M* methenamine, and 2 mL (concentration in reaction bath is about 0.25 at.%) of ZnO sol were mixed at room temperature, and the substrate was suspended in the solution, and heated at 95°C for 1 h. Finally, the prepared samples were washed by deionized water and dried at 100°C for 1 h.

(4) Characterization

The phase composition of the samples was characterized by X-ray powder diffraction (XRD, RINT-2100V, Rigaku, Tokyo, Japan; Cu$K\alpha$). The morphologies of the samples were observed by field emission scanning electron microscopy (FESEM; JSM-6335FM, JEOL, Tokyo, Japan; with an accelerating voltage of 5 kV).

III. Results and Discussion

Figure 1 shows the SEM images of ZnO nanotubes by selective etching of ZnO rods, where hexagonal ZnO nanotubes with a uniform wall thickness of several tens of nanometers and an external diameter of 500 nm are observed. Most of the ZnO nanotubes are predominantly aligned perpendicular to the substrate, and from the nanotubes aligned horizontal to the substrate the length of the nanotubes was calculated to be about 1 μm. Besides, the nanotubes are densely aligned and some coalesce together.

Considering that the nanotubes were obtained from ZnO rods, their morphology would be considerably affected by the fabrication condition of ZnO rods. From the former research about the chemical bath-deposited ZnO rod arrays, we have found that the seed layer plays a key role in their crystallinity and morphology.[30] Figure 2 shows the morphology of ZnO nanotubes prepared using different seed layers. When the seed layer is heated at 150°C for 10 min, tubular structures are also formed, as shown in Figs. 2(a) and (b). It should be noted that only the upper part of the rod is hollow, while the lower part still remains dense. Interestingly, there are small holes in the inner center of some nanotubes. The presence of the holes indicates that on the (0001) surface, the etching process of the center is faster than that of the edge. On further increasing the heating temperature of the seed layer to 300°C, the nanotubes became denser and no holes were found in the nanotubes. As shown in Fig. 2(c), the outer diameter is increased.

Basically, the selective dissolution mechanism is applied to explain the formation of a ZnO tubular structure. It is believed that the Zn-terminated polar face (0001) is metastable and chemically active.[21] Therefore, the etching rate of the (0001) face is much faster than that of the side faces, resulting in the dissolution of the rod core from the tip to the bottom and the formation of a hollow structure. In this mechanism of etching, the intrinsic defects produced during ZnO rod preparation play an important role in the formation of a hollow structure. As a result, the morphology evolution of the ZnO nanotubes obtained from different seed layers can be explained by the fact that if the seed layer is heated at high temperatures (e.g. 300°C), the as-prepared ZnO rod arrays will have better crystal quality and a low concentration of defects.[28] Thus, only the upper part of the rods could be etched.

It is worth noting that the addition of Al^{3+} ions in the precursor would also affect the structure of the final product. Figure 3 shows the SEM images of the sample in the absence of Al^{3-} ions. It can be seen from Fig. 3(a) that the sample is composed of a nonoriented rod-like structure, and most of the rods are not hollow, with an average diameter of 130 nm. One should notice that there would be some difference in the pH value between the precursor solution of ZnO rods with and without Al^{3+} ions. For the precursor solution without Al^{3+} ions, the initial pH value is about 6.7 before chemical bath deposition. As to the solution that contains 2 at.% aluminum nitrite, the pH value decreases to about 6.1. Therefore, a pH 6.1 precursor solution without Al^{3+} ions was prepared by adding HAc, and the morphology of the product after etching is shown in Fig. 3(b), where plate-assembled films instead of a tubular structure are found. The results indicate that the presence of Al^{3+} ions is crucial to the formation of a tubular structure. In order to investigate the role of Al^{3-} ions, the dependence of Al^{3+} ions on the morphology of ZnO rods has been studied previously. As shown in Supporting information Fig. S1, it can be seen that the pure film consists of agglomerated particles, while the film with addition of aluminum shows a rod-like morphology.

According to the selective dissolution mechanism, the formation of a ZnO tubular structure is caused by the difference in the dissolution rate between the top and the side surface of ZnO rods. For a dense ZnO film, the selective dissolution seems unlikely because of a small side surface. The addition of Al^{3+} may have two main effects on the structure of ZnO films. First, the Al^{3+} ions in the precursor solution could act as an impurity to prevent the combination process of ZnO rods. Second, because the typical ZnO crystal exhibits a polar (0001) surface, a certain amount of Al^{3-} ions can be adsorbed on the (0001) surface, inducing the high density of defects on this surface. Previous work suggested that the adsorption of foreign ions plays a major role in the formation of ZnO nanotubes. For example, for electrodeposited ZnO nanowires obtained from $ZnCl_2$, Cl^- ions might be preferentially adsorbed on the top of the nanowires, resulting in the formation of a highly water-soluble zinc chloride complex.[21]

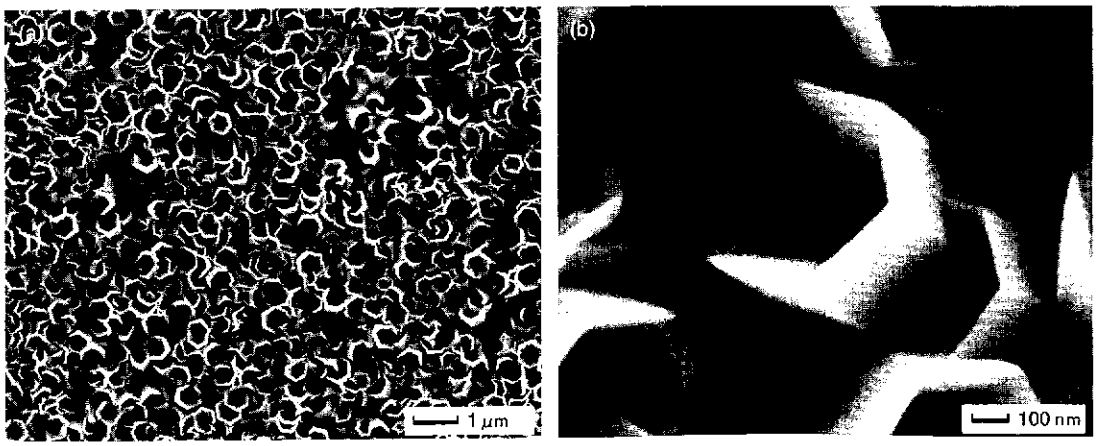

Fig. 1. Scanning electron microscopic images of ZnO nanotubes by selective etching of ZnO rods in 0.3*M* KOH aqueous solution for 60 min.

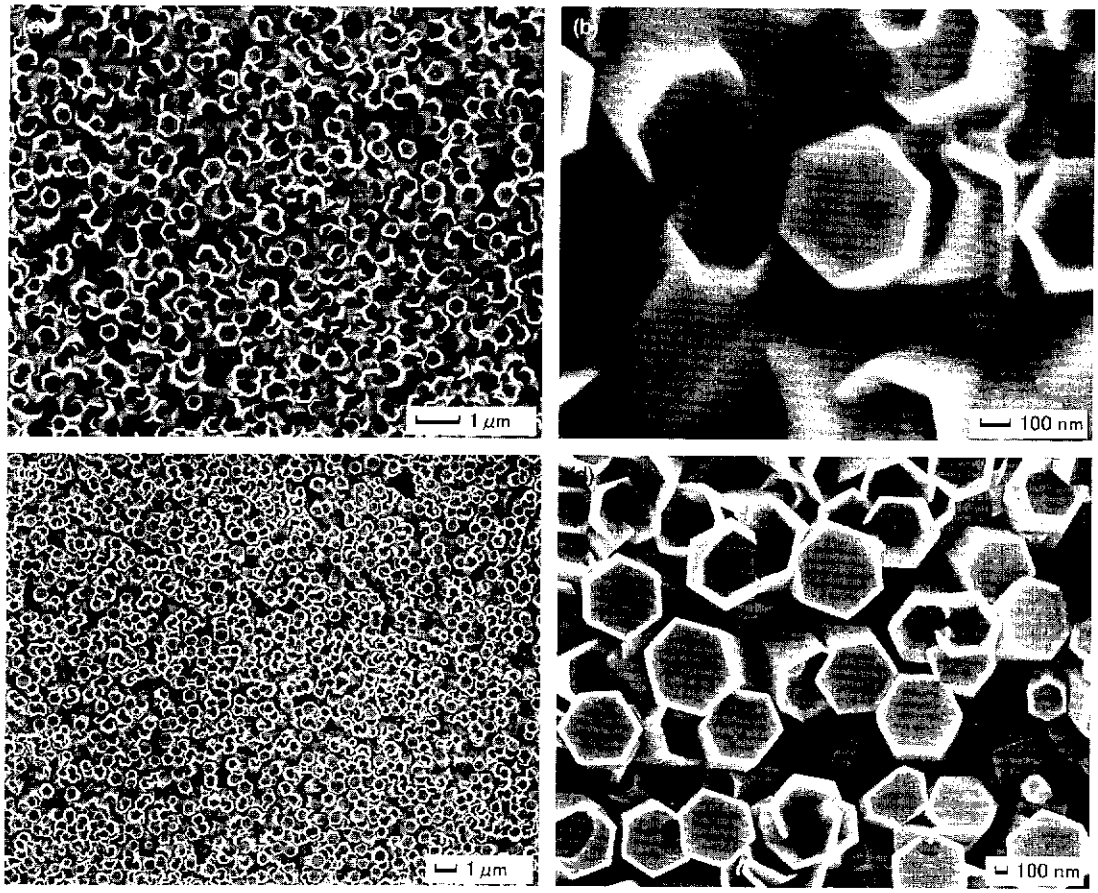

Fig. 2. Scanning electron microscopic images of ZnO nanotubes prepared using different seed layers: (a, b) the seed layer was heat treated at 150°C for 10 min; (c, d) the seed layer was heat treated at 300°C for 30 min.

Thus, the nanowires' core could be gradually dissolved in KCl solution and then nanotubes were obtained. However, this method might be not suitable for chemical bath deposition. It was reported that by increasing the content of KCl in the precursor solution, the morphology of ZnO changed from 1D ZnO nanorod arrays to 2D dense films.[31] The defect selective mechanism is further supported by annealing ZnO rods with 2 at.% Al in air at 300°C for 2 h and then equal etching under the same condition. It was found that the annealed ZnO rods could not be etched into nanotubes. The reason for this phenomenon might be that upon annealing, the defects in ZnO would attain a thermal equilibrium with a uniform distribution instead of preferentially locating at the center of ZnO rods.[19] Therefore, no preferential etching would occur from the center to form a tubular structure. Further, the feasibility of forming a ZnO tubular structure is sensitive to the diameter of the previously deposited rods. Supporting information Fig. S2 shows the SEM images of the etched sample obtained from thin ZnO rods, where no tubular structure can be observed. This is not surprising as the small diameter means less area of the (0001) surface, resulting in less energy difference between the top and the side surfaces. Efforts to increase the diameter of ZnO rods, such as increasing the Zn^{2+} concentration and growth time, are not favorable for fabrication of nanotubes because increasing the diameter simultaneously increases the possibility of combination of neighboring rods. The above investigation indicates that adding Al^{3+} ions is an effective way to obtain ZnO nanotube arrays in an aqueous solution. In addition, it is another issue whether Al^{3+} ions have been incorporated into ZnO crystal lattices. Figure 4(a) shows the XPS full spectra of 2 at%

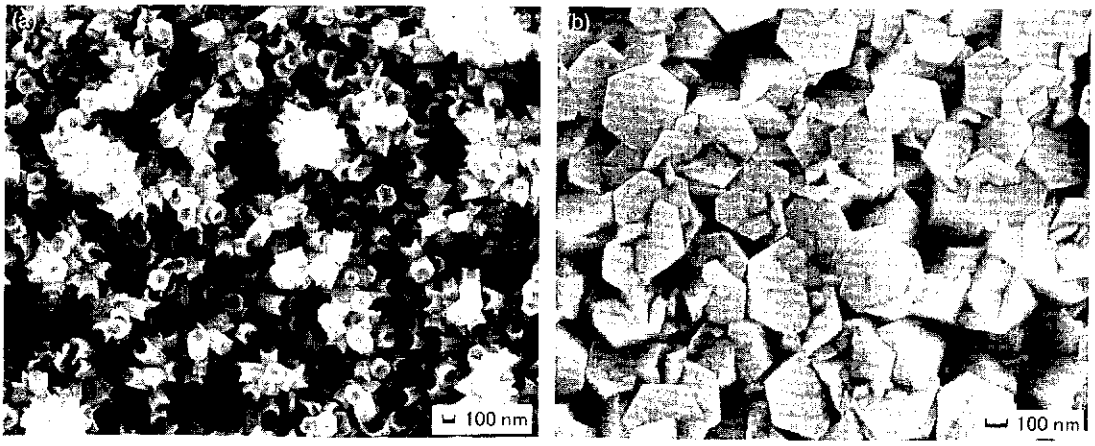

Fig. 3. Scanning electron microscopic images of etched ZnO samples prepared without adding Al^{3+} ions. (a) Precursor solution pH 6.7; (b) pH 6.1.

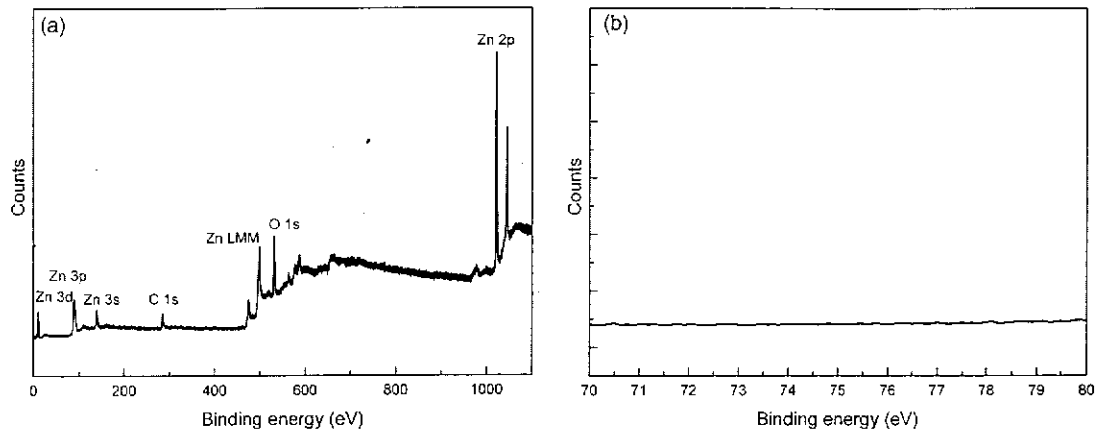

Fig. 4. XPS spectra of ZnO rods prepared with 2 at% Al^{3+} ion doping. (a) full spectrum; (b) Al $2p_{3/2}$.

Al-doped ZnO rods, where the binding energies were calibrated by considering the C 1*s* peak as a reference. XPS peaks at ~1022.6 and ~1045.8 eV corresponding to the $2p_{3/2}$ and $2p_{1/2}$ core levels of Zn in ZnO, as well as peaks at ~531.6 eV attributed to O 1*s* can be observed, while the peak of Al that usually appears near the binding energy of 74.17 eV, Al $2p_{3/2}$, is not found. The XPS results indicate that Al^{3+} has not been incorporated into ZnO crystal lattices, which might be due to the fact that the diffusion of Al in ZnO is negligible at a low temperature.

Figure 5 shows the SEM images of ZnO nanoflowers grown with the addition of 2 mL ZnO sol. As shown in Fig. 5(a), the as-prepared ZnO is composed of a bilayer structure, and the upper layer is made of nanorod-based flower-like structures. From Fig. 5(b), it can clearly be seen that the single nanoflower is about 800 nm in size with many nanorods growing radially from the center in symmetry, and most of the nanoflowers are connected to each other. Also, the bottom layer is composed of a nanorod array. It is noticeable that the size of the as-prepared nanoflowers is much smaller than those reported, which might result from a relatively low pH value (~6).[16] Correspondingly, the average diameter of nanorods in nanoflower is <50 nm, and the smaller size may favor a higher surface area. Further, from Fig. 5(c), the sharp tip of the nanorods can be observed. To make the bottom layer clear, cross-section SEM images are observed. As shown in Fig. 5(d), the nanorods are oriented on the substrate with ~200 nm length and ~40 nm diameter. The nanoflower layer is uniformly covered on the surface of nanorod arrays.

It was found that introducing ZnO sol into the reaction solution plays a key role in the formation of ZnO nanoflowers.

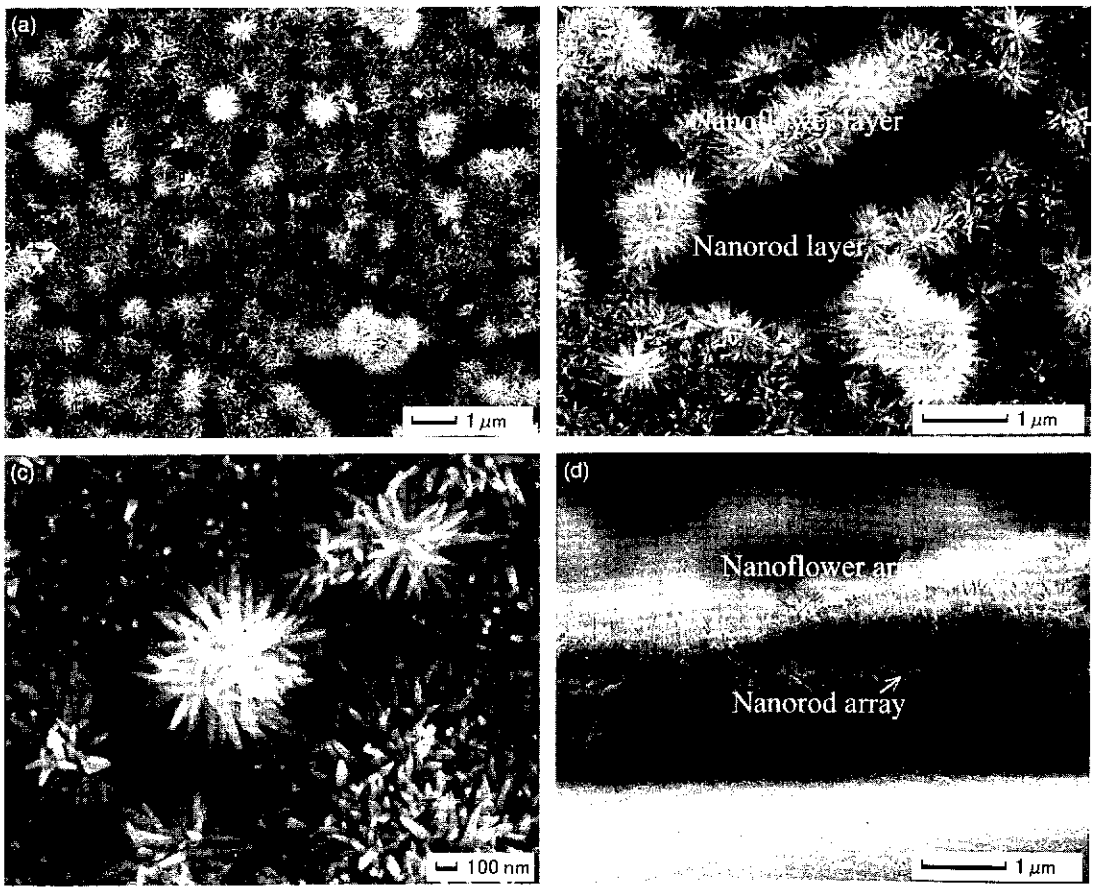

Fig. 5. Scanning electron microscopic images of as-prepared ZnO nanoflowers. (a–c) show top views of the sample; (d) shows the cross-section image.

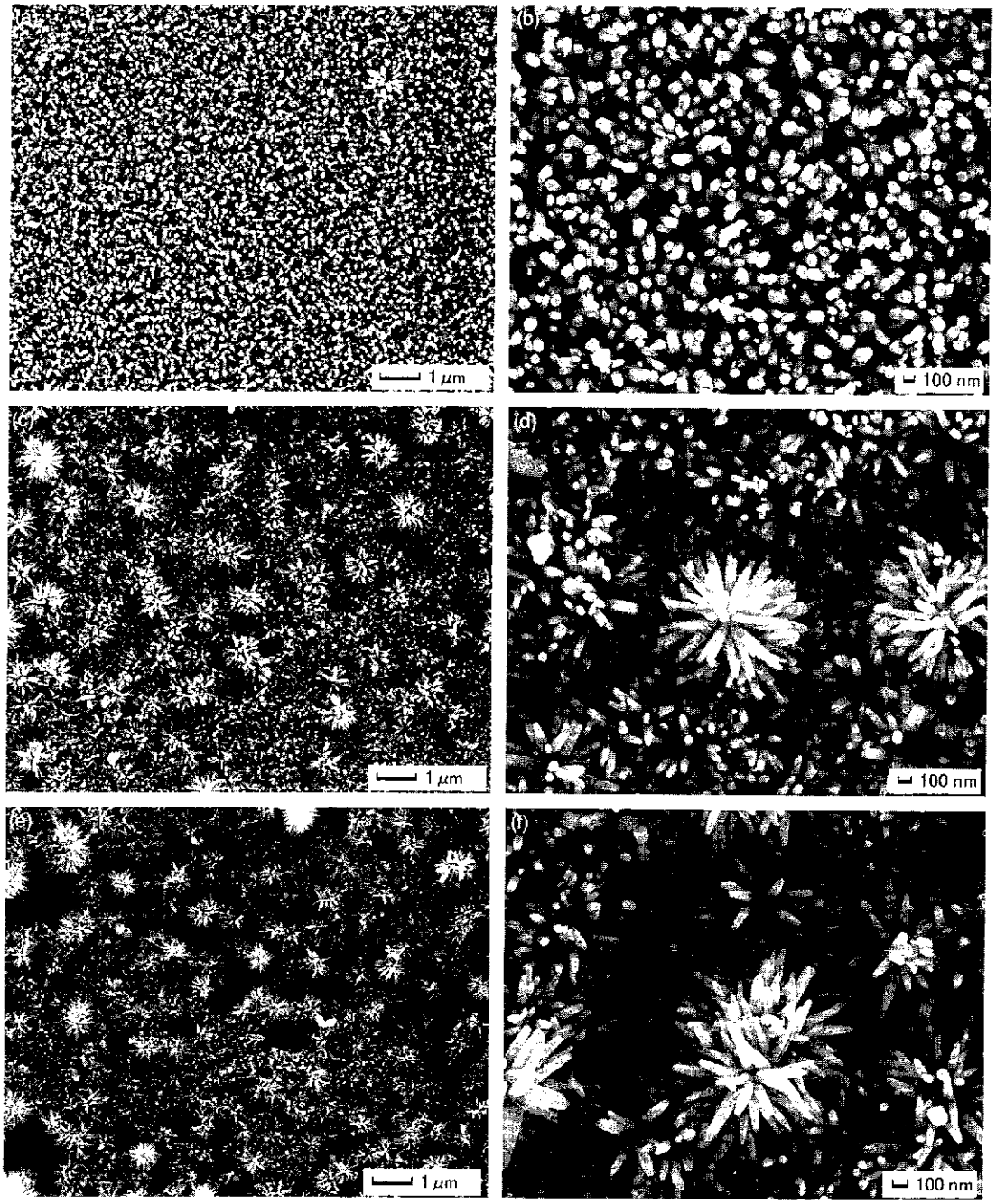

Fig. 6. Scanning electron microscopic images of ZnO nanostructures with different amounts of ZnO sol. (a, b) 0 mL sol; (c, d) 1 mL; (e; and f) 3 mL.

Figure 6 displays the as-prepared ZnO nanostructures with different amounts of ZnO sol addition. Without adding ZnO sol, only well-oriented nanorod arrays are obtained, as shown in Figs. 6(a) and (b). The average diameter of the nanorod is about 80 nm, which is larger than that of the bottom layer of nanoflowers. The average length of the nanorods is also obviously increased. When 1 mL ZnO sol is introduced, some flower-shaped ZnO nanostructures are formed, and the nanoflowers are distributed randomly on the nanorod layer. As the ZnO sol is increased to 3 mL, a dense nanoflower layer can be observed in Figs. 6(e) and (f), while the dimension of individual nanoflowers remains almost constant. Further, the crystal structures of the nanoflowers with different ZnO sol additions are examined by XRD, which is shown in Fig. 7. It can be found that the (0002) peak intensity gradually decreases with increasing ZnO sol content, indicating less alignment.

Following the experimental observations, the growth of a ZnO nanoflower is schematically summarized in Fig. 8. When a seeded substrate is immersed into a hot solution of zinc nitrate and methenamine, homogeneous precipitation of ZnO occurs and rod-like array structures are formed. At the same time, if ZnO sol is added to the reaction solution, ZnO nanoparticles in sol will be randomly distributed into the solution. As a result, homogeneous nucleation also occurs on these nanoparticles, and rod-like structures are formed around them. Different from the nanorod array on the substrate, these rod-like structures grow with random directions due to the absence of a substrate. Meanwhile, some amount of the ZnO nanoparticles would be adsorbed on the tip of the nanorod array. This is because the tip of the ZnO nanorod usually possesses a charged polar (0001) surface. The adsorption of nanoparticles onto the (0001) ZnO surface may result in the formation of randomly oriented flower-shaped nanostructures on the top of the nanorod, as shown in Fig. 6(c). With a further increase in the content of the ZnO sol, the formed ZnO nanoflowers will be self-assembled into a large-scale network to decrease the surface energy and a

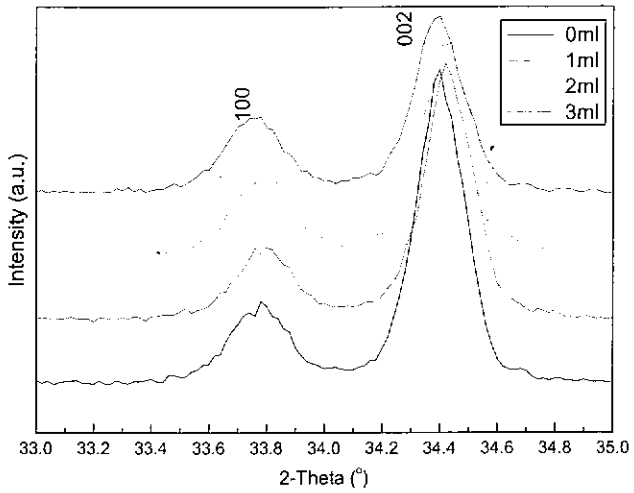

Fig. 7. X-ray diffraction patterns of ZnO nanostructures with different amounts of ZnO sol.

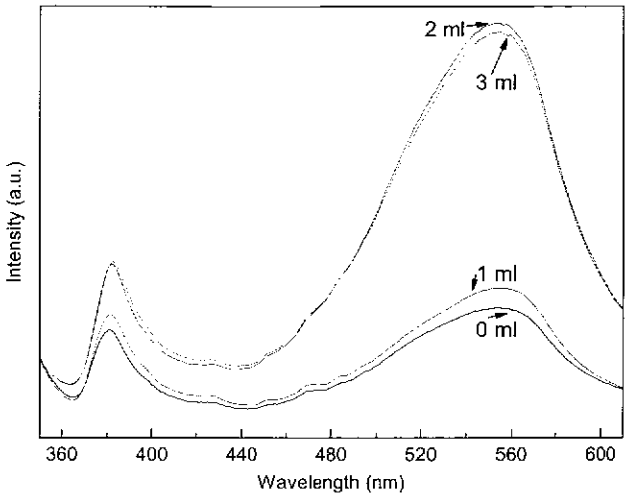

Fig. 9. Room-temperature PL spectra of ZnO nanoflowers with different amounts of ZnO sol.

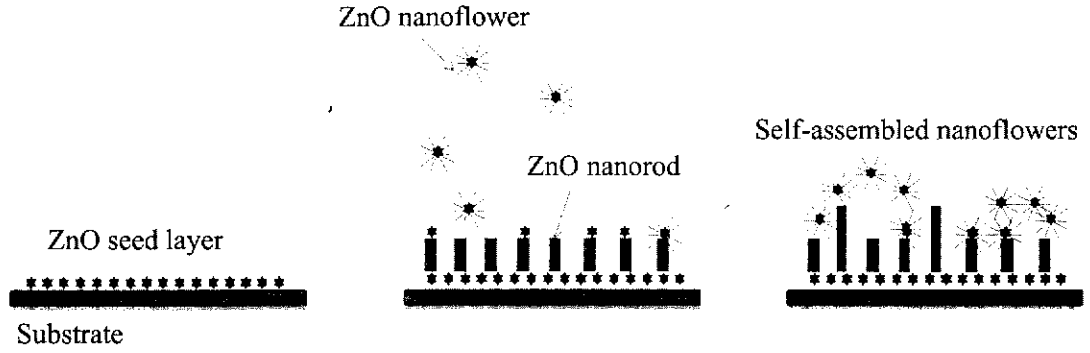

Fig. 8. Schematic view of ZnO nanoflowers' growth process.

bilayer structure is obtained. In this structure, the growth of the bottom nanorod layer is suppressed considerably, which results from the fact that the nanoparticles on the surface act as nuclei for growing crystals.

The optical property of as-synthesized ZnO nanoflowers is investigated here. Figure 9 shows their room-temperature photoluminescence spectra. For all the samples, there are two emission bands for ZnO that center at the UV and the visible range, respectively. The UV emission is the intrinsic near-band-gap emission that can be attributed to the recombination of free excitons, while the origin of the visible emission can be ascribed to intrinsic defects and impurities (including adsorbed oxygen, hydroxide, moisture, etc.). After adding ZnO sol, the visible emission is significantly enhanced. Noting that the growth conditions (pH, temperature, time, etc.) of ZnO remain almost the same with addition of ZnO sol, it is believed that the stronger visible emission is caused by the more adsorbed oxygen. This is reasonable, considering that the surface area of nanoflowers is larger than that of nanorod arrays, and the larger the surface, the more oxygen can be adsorbed. However, if the whole nanorod array is covered by ZnO nanoflowers, the increase of the surface area is limited. Thus, the nanoflowers with addition of 2 and 3 mL ZnO sol show similar intensities of visible emission.

IV. Conclusion

In summary, we have demonstrated a facile approach to synthesize a ZnO nanotube array and nanoflowers in an aqueous solution. Detailed characterization of as-prepared ZnO nanostructures has been carried out. For ZnO nanotubes, the presence of Al^{3+} ions plays a crucial role in the formation of a tubular structure, and ZnO nanotubes with different inner structures are obtained by varying the seed layers. By introducing ZnO sol into the reaction solution, a bilayer ZnO nanostructure consisting of a ZnO nanorod array at the bottom and nanoflowers at the top can be fabricated. The ZnO nanoflowers are self-assembled and show unique optical properties. The present route allows the fabrication of different ZnO nanostructures by simply controlling additives.

Supporting Information

Additional Supporting Information may be found in the online version of this article:

Figure S1. SEM images of ZnO rods array obtained from CBD with different amount of Al: (a) 0 at.%; (b) 2 at.%.

Figure S2. SEM image of ZnO after etching, the chemical bath deposition temperature is 90°C, and growth time is 1 h.

Figure S3. XRD patterns of ZnO nanotubes prepared using different seed layers.

Please note: Wiley-Blackwell are not responsible for the content or functionality of any supporting materials supplied by the authors. Any queries (other than missing material) should be directed to the corresponding author for the article.

References

[1]J. Rousset, E. Saucedo, and D. Lincot, "Extrinsic Doping of Electrodeposited Zinc Oxide Films by Chlorine for Transparent Conductive Oxide Applications," *Chem. Mater.*, **21** [3] 534–40 (2009).

[2]A. Suzuki, M. Nakamura, R. Michihata, T. Aoki, T. Matsushita, and M. Okuda, "Ultrathin Al-Doped Transparent Conducting Zinc Oxide Films Fabricated by Pulsed Laser Deposition," *Thin Solid Films*, **517** [4] 1478–81 (2008).

[3]T. Yamazaki, S. Wada, T. Noma, and T. Suzuki, "Gas-sensing Properties of Ultrathin Zinc Oxide Films," *Sens. Actuators B*, **13–14**, 594–5 (1993).

[4]K. Keis, L. Vayssieres, S. E. Lindquist, and A. Hagfeldt, "Nanostructured ZnO Electrodes for Photovoltaic Applications," *Nanostruct. Mater.*, **12** [1–4] 487–90 (1999).

[5]T. Pauporte and D. Lincot, "Electrodeposition of Semiconductors for Optoelectronic Devices: Results on Zinc Oxide," *Electrochimica Acta*, **45** [20] 3345–53 (2000).

[6]B. B. Jason and S. A. Eray, "Nanowire-Based Dye-Sensitized Solar Cells," *Appl. Phys. Lett.*, **86** [5] 053114, 3pp (2005).

[7]M. Law, L. E. Greene, J. C. Johnson, R. Saykally, and P. D. Yang, "Nanowire Dye-sensitized Solar Cells," *Nat. Mater.*, **4** [6] 455–9 (2005).

[8]K. Govender, D. S. Boyle, P. B. Kenway, and P. O'Brien, "Understanding the Factors that Govern the Deposition and Morphology of Thin Films of ZnO from Aqueous Solution," *J. Mater. Chem.*, **14** [16] 2575–91 (2004).

[9]J. Yang, J. Lang, C. Li, L. Yang, Q. Han, Y. Zhang, D. Wang, M. Gao, and X. Liu, "Effects of Substrate on Morphologies and Photoluminescence Properties of ZnO Nanorods," *Appl. Surf. Sci.*, **255** [5, Part 1] 2500–3 (2008).

[10]M. Wang and L. Zhang, "The Influence of Orientation on the Photoluminescence Behavior of ZnO Thin Films Obtained by Chemical Solution Deposition," *Mater. Lett.*, **63** [2] 301–3 (2009).

[11]S. Yamabi and H. Imai, "Growth Conditions for Wurtzite Zinc Oxide Films in Aqueous Solutions," *J. Mater. Chem.*, **12** [12] 3773–8 (2002).

[12]B. D. Yuhas and P. Yang, "Nanowire-Based All-Oxide Solar Cells," *J. Am. Chem. Soc.*, **131** [10] 3756–61 (2009).

[13]T. Oekermann, T. Yoshida, H. Tada, and H. Minoura, "Color-Sensitive Photoconductivity of Nanostructured ZnO/Dye Hybrid Films Prepared by One-Step Electrodeposition," *Thin Solid Films*, **511–512**, 354–7 (2006).

[14]J. B. Baxter and E. S. Aydil, "Dye-Sensitized Solar Cells Based on Semiconductor Morphologies with ZnO Nanowires," *Solar Energy Mater. Solar Cells*, **90** [5] 607–22 (2006).

[15]J. Zhao, D. Wu, and J. Zhi, "A Novel Tyrosinase Biosensor Based on Biofunctional ZnO Nanorod Microarrays on the Nanocrystalline Diamond Electrode for Detection of Phenolic Compounds," *Bioelectrochemistry*, **75** [1] 44–9 (2009).

[16]C. Y. Jiang, X. W. Sun, G. Q. Lo, D. L. Kwong, and J. X. Wang, "Improved Dye-Sensitized Solar Cells with a ZnO-Nanoflower Photoanode," *Appl. Phys. Lett.*, **90** [26] 263501–3 (2007).

[17]X. H. Zhang, S. Y. Xie, Z. Y. Jiang, X. Zhang, Z. Q. Tian, Z. X. Xie, R. B. Huang, and L. S. Zheng, "Rational Design and Fabrication of ZnO Nanotubes from Nanowire Templates in a Microwave Plasma System," *J. Phys. Chem. B*, **107** [37] 10114–8 (2003).

[18]Q. C. Li, V. Kumar, Y. Li, H. T. Zhang, T. J. Marks, and R. P. H. Chang, "Fabrication of ZnO Nanorods and Nanotubes in Aqueous Solutions," *Chem. Mater.*, **17** [5] 1001–6 (2005).

[19]G. W. She, X. H. Zhang, W. S. Shi, X. Fan, J. C. Chang, C. S. Lee, S. T. Lee, and C. H. Liu, "Controlled Synthesis of Oriented Single-Crystal ZnO Nanotube Arrays on Trenasparent Conductive Substrates," *Appl. Phys. Lett.*, **92**, 053111, 3pp (2008).

[20]Y. Sun, N. G. Ndifor-Angwafor, D. J. Riley, and M. N. R. Ashfold, "Synthesis and Photoluminescence of Ultra-thin ZnO Nanowire/nanotube Arrays Formed by Hydrothermal Growth," *Chem. Phys. Lett.*, **431** [4–6] 352–7 (2006).

[21]J. Elias, R. Tena-Zaera, G.-Y. Wang, and C. Lévy-Clément, "Conversion of ZnO Nanowires into Nanotubes with Tailored Dimensions," *Chem. Mater.*, **20** [21] 6633–7 (2008).

[22]L. Vayssieres, K. Keis, A. Hagfeldt, and S.-E. Lindquist, "Three-Dimensional Array of Highly Oriented Crystalline ZnO Microtubes," *Chem. Mater.*, 13 [12] 4395–8 (2001).

[23]X. Gan, X. Li, X. Gao, and W. Yu, "Investigation on Chemical Etching Process of ZnO Nanorods Toward Nanotubes," *J. Alloys Compd.*, **481** [1–2] 397–401 (2009).

[24]A. L. Pan, R. C. Yu, S. S. Xie, Z. B. Zhang, C. Q. Jin, and B. S. Zou, "ZnO Flowers Made up of Thin Nanosheets and their Optical Properties," *J. Cryst. Growth*, **282** [1–2] 165–72 (2005).

[25]Z. Wang, X. F. Qian, J. Yin, and Z. K. Zhu, "Large-Scale Fabrication of Tower-Like, Flower-Like, and Tube-Like ZnO Arrays by a Simple Chemical Solution Route," *Langmuir*, **20** [8] 3441–8 (2004).

[26]H. Zhang, D. Yang, Y. J. Ji, X. F. Ma, J. X, and D. L. Que, "Low Temperature Synthesis of Flowerlike ZnO Nanostructures by cetyltrimethylammonium Bromide-Assisted hydrothermal Process," *J. Phys. Chem. B*, **108**, 3955–8 (2004).

[27]Z. Fang, K. Tang, G. Shen, D. Chen, R. Kong, and S. Lei, "Self-assembled ZnO 3D Flowerlike Nanostructures," *Mater. Lett.*, **60** [20] 2530–3 (2006).

[28]F. Xu, K. Yu, G. D. Li, Q. Li, and Z. Q. Zhu, "Synthesis and Field Emission of Four Kinds of ZnO Nanostructures: Nanosleeve-fishes, Radial Nanowire Arrays, Nanocombs and Nanoflowers," *Nanotechnology*, **17** [12] 2855–9 (2006).

[29]L. Spanhel and M. A. Anderson, "Semiconductor Clusters in the Sol gel Process: Quantized Aggregation, Gelation, and Crystal Growth in Concentrated Zinc Oxide Colloids," *J. Am. Chem. Soc.*, **113** [8] 2826–33 (1991).

[30]D. Chu, T. Hamada, K. Kato, and Y. Masuda, "Growth and Electrical Properties of ZnO Films Prepared by Chemical Bath Deposition Method," *Physica Status Solidi A*, **206** [4] 718–23 (2009).

[31]J. Qiu, X. Li, W. Yu, X. Gao, W. He, S.-J. Park, Y.-H. Hwang, and H.-K. Kim, "Morphology Transformation from ZnO Nanorod Arrays to ZnO Dense Film Induced by KCl in Aqueous Solution," *Thin Solid Films*, **517** [2] 626–30 (2008).